



Detection of 16 Small Glitches in Nine Pulsars

Zu-Rong Zhou^{1,2}, Jing-Bo Wang^{1,3,4}, Na Wang^{1,3,4}, Jian-Ping Yuan^{1,3,4}, Fei-Fei Kou^{1,3,4}, and Shi-Jun Dang⁵

¹ Xinjiang Astronomical Observatory, Chinese Academy of Sciences, Urumqi 830011, China; wangjingbo@xao.ac.cn, na.wang@xao.ac.cn

² University of Chinese Academy of Sciences, Beijing 100049, China

³ Xinjiang Key Laboratory of Radio Astrophysics, Urumqi 830011, China

⁴ Key Lab of Radio Astronomy, Chinese Academy of Sciences, Beijing 100101, China

⁵ School of Physics and Electronic Science, Guizhou Normal University, Guiyang 550001, China

Received 2022 May 22; accepted 2022 June 21; published 2022 August 10

Abstract

Pulsar timing measurements with a 26 m radio telescope at Nanshan between 2000 and 2014 were used to search for glitch events. The data span of nine pulsars ranges from 11.6 to 14.2 yr, and 16 new glitch events were identified in nine pulsars. Glitch parameters were determined through fitting the timing residuals data. All 16 glitches have a small fractional size. Six new glitches have been detected in PSR J1833–0827, making it another frequent glitching pulsar. Some of the 16 glitches may experience exponential or linear recovery, but it is unlikely for us to make further analyses with the large gap in the data set. All the glitch rates obtained from Nanshan are higher than that from Jodrell Bank Observatory. The small glitch size and high glitch rate could possibly attribute to the high observation cadence.

Key words: stars: neutron – methods: data analysis – (stars:) pulsars: general

1. Introduction

Radio pulsars are considered to be remarkably stable rotators, which can be used to establish a pulsar timescale (Kramer et al. 2021), search for ultra-low frequency gravitational waves (Shannon & Cordes 2017; Hobbs et al. 2019) and proves of general relativity (Kramer et al. 2006). These results all depended on the so-called pulsar timing technique (Yu et al. 2013). Details of the pulsar timing technique are described in Hobbs et al. (2009). The critical quantity of the pulsar timing technique is the times-of-arrival (ToAs) of the observed pulses, which are always made a comparison with predictive ToAs. The speculative ToAs are measured by a theoretical model of the pulsar’s position, rotation, etc. The numerical differences between the predicted and the actual ToAs are described as the pulsar timing residuals (Shaw et al. 2018). For an ideal model, the residuals of timing would be dominant by errors in measurement and have a white spectrum (Groth 1975). Any characteristics seen in the residuals imply the existence of unmodelled influences, which might contain calibration errors, irregularities of spin-down, or orbital companions (Kerr et al. 2020).

Two main types of timing irregularity have been recognized: timing noise and glitches. The physical processes behind both phenomena are not well understood. Timing noise is an unmodelled feature in the residuals of timing relative to a simple slowdown model (Cordes & Shannon 2010) and has been seen in all classes of pulsars (Parthasarathy et al. 2019). It could be described as a random walk of the residuals, sometimes exhibiting a clear quasi-periodic behavior (Hobbs et al. 2010).

Some of these characteristics have been shown to come into being in instabilities in the magnetosphere of a pulsar, which lead to state changes in the spin-down rate (Lyne et al. 2010). A glitch is an abrupt increase in frequency of a neutron star (NS), and the detected fractional glitch size range from $\sim 10^{-12}$ to $\sim 10^{-5}$ with a bimodal distribution (Yu et al. 2013). Glitches are unpredictable and rare events and vary vital for different pulsars (Espinoza et al. 2011). A majority of glitches are detected in relatively younger pulsars, but were also observed in millisecond pulsars (MSP) and magnetars (Kaspi & Beloborodov 2017). Pulsar sometimes enters a recovery process following a glitch, in which the rotation frequency decays toward the pre-glitch value. The glitch recovery can be explained as a signature of the existence of a superfluid in the interior of the pulsar (Baym & Pethick 1996). A better understanding of glitches will provide a probe to the internal structure of NS. Glitches are thought to be triggered either with the abrupt shift of angular momentum from the crustal superfluid of a faster-rotating speed to the rest of the NS (Chamel 2013) or by the NS crustquakes (Bransgrove et al. 2020). The exponential recoveries can be interpreted as the reconstruct of equilibrium between unpinning and pinning in a vortex-creep region interior to an NS (Gügercinoğlu & Alpar 2014). More than fifty years after the discovery of the first glitch, the exact origin of these phenomena is not yet well understood (Haskell & Melatos 2015).

This paper presents the outcomes of a new search for glitch evens performed with the Nanshan pulsar timing database. Sixteen new glitches detected in this work are applied with studying the glitching behavior of pulsars. We describe our

observations in Section 2. Our results are shown in Section 3. We discuss the results and conclude the paper in Sections 4 and 5, respectively.

2. Observation and Data Analysis

Timing observations of the nine pulsars at Xinjiang Astronomical Observatory (XAO) are executed with the 26 m telescope at Nanshan (Wang et al. 2001). A normal temperature receiver was used since 1999 and updated to a cryogenic system in 2002 July. The bandwidth of the receiver is 320 MHz, and its center frequency is 1540 MHz. Before 2010, an analog filter bank (AFB) with 1282.5 MHz sub-channels was used to take data. After 2010 January, the data were obtained by a digital filterbank system (DFB) with 1024 channels. These nine pulsars have been usually observed three times per month, and the presented timing data were gathered between 2000 January 4th, and 2014 March 4th. Observation's integration times for each pulsar are from 4 to 16 minutes.

The PSRCHIVE software package (Hotan et al. 2004) is applied with offline data reduction. An initial set of pulsar parameters is achieved from the ATNF pulsar catalog (Manchester et al. 2005). After dedispersing and removing radio-frequency interference (RFI), the data are summed in time, polarization, and frequency to produce an integration profile. A standard template is obtained by fitting single or multiple Gaussian components to the integration profile. The template is then cross-correlated with each observing to obtain pulse ToAs. Then, the TEMPO2 (Hobbs et al. 2006) software package is used to turn the topocentric ToAs into the arrival times at the solar system barycentre with the Jet Propulsion Laboratory (JPL) planetary ephemeris DE421 (Folkner et al. 2009). All observed ToAs were contrasted with terrestrial time (TT) as achieved by the international atomic time (TAI).

The pulse phase (Φ) predicted by a standard timing model can be stated as:

$$\Phi(t) = \Phi_0 + \nu(t - t_0) + \frac{1}{2}\dot{\nu}(t - t_0)^2 + \frac{1}{6}\ddot{\nu}(t - t_0)^3, \quad (1)$$

where Φ_0 is the pulse phase at the time t_0 , ν , $\dot{\nu}$ and $\ddot{\nu}$ are the rotational frequency and its derivatives respectively.

The increased pulse phase caused by a glitch is described as:

$$\begin{aligned} \Delta\Phi_g &= \Delta\Phi + \Delta\nu_p(t - t_g) + \frac{1}{2}\Delta\dot{\nu}_p(t - t_g)^2 \\ &+ [1 - e^{-(t-t_g)/\tau_d}]\Delta\nu_d\tau_d, \end{aligned} \quad (2)$$

where glitch can be described using an offset in phase $\Delta\Phi$ and the permanent incremental quantities in the frequency $\Delta\nu_p$ and its first frequency derivative $\Delta\dot{\nu}_p$, in addition to a temporary frequency incremental quantity $\Delta\nu_d$ which decreases exponentially with a timescale τ_d . Glitch epoch (t_g) was estimated to be halfway between the first post-glitch measurement and the last pre-glitch measurement. The variations in the frequency and

first derivative of frequency at the glitch can be expressed as

$$\Delta\nu_g = \Delta\nu_p + \Delta\nu_d, \quad (3)$$

and

$$\Delta\dot{\nu}_g = \Delta\dot{\nu}_p - \frac{\Delta\nu_d}{\tau_d}, \quad (4)$$

respectively. In addition, the recovery degree can be described by:

$$Q = \Delta\nu_d/\Delta\nu_g. \quad (5)$$

The signature of a glitch event in plots of timing residuals and frequency with epoch has been demonstrated in Figure 1 of Espinoza et al. (2011). In this work, all glitches in this paper were found by visual inspection of the phase residuals. Any feature looking like those in Figure 1 of Espinoza et al. (2011) was regarded as a glitch candidate and explored at length.

3. Results

We have found 16 new glitches in nine pulsars. Compared with Basu et al. (2022) and Lower et al. (2021), most glitches detected in this work have small fractional size ($\Delta\nu_g/\nu \leq 10^{-9}$). Table 1 concludes the parameters of each detected glitch. The first two columns list the pulsar name and the reference number for each detected glitch. The third column shows the glitch epoch with each uncertainty in parentheses. The fourth and the fifth columns list the relatively varieties in the frequency and its first-time derivative. The root means square of residuals, data span, number of TOAs, and characteristic ages are separately given in the rest of the columns. Except for the glitch epoch, all uncertainties are quoted at the 1σ level returned by TEMPO2. The uncertainty of the glitch epoch was fixed a quarter of the observation gap between the last pre-glitch observation and the first post-glitch measurement. In Table 1, all these pulsars have been observed with glitches before (Yuan et al. 2010; Espinoza et al. 2011; Yu et al. 2013; Lower et al. 2021; Basu et al. 2022). There are 10 glitches reported in Lower et al. (2021) and Basu et al. (2022) were also detected by us. It is not necessary to repeat their results here.

3.1. PSR J0528+2200 (B0525+21)

This pulsating radio source was found near the Crab Nebula (Staelin & Reifenstein 1968). It is a very long-period pulsar with $P=3.746$ s. In total, four small glitches had been addressed for PSR J0528+2200 (Downs 1982; Shemar & Lyne 1996; Janssen & Stappers 2006; Yuan et al. 2010). We identified a new tiny glitch at MJD $\sim 54,931$ with a fractional size of $\Delta\nu/\nu=0.21 \times 10^{-9}$, which is comparable with the glitch reported by Janssen & Stappers (2006) at MJD 53,379. It is possible that a linear decrease of frequency relative to the pre-glitch solution lasts for at least 200 days and an over-recovery of frequency ν after glitch. This is similar to the behavior detected in the Crab pulsar (Lyne et al. 1993).

Table 1
Glitch Parameters of the 16 New Glitches

Pulsar Name	Gl. No.	Epoch (MJD)	$\Delta\nu/\nu$ (10^{-9})	$\Delta\dot{\nu}/\dot{\nu}$ (10^{-3})	rms res. (μ s)	Data Span (MJD)	No. of TOAs	Age (Myr)
J0528+2200	1	54,931.0(3)	0.21(4)	1.0(2)	488.634	54,007–55,263	160	1.48
J1705–3423	1	55 490(13)	0.28(1)	0.11(7)	636.888	54,450–56,718	197	3.76
J1833–0827	1	51871(1)	0.22(2)	0.02(1)	134.933	51,550–52,262	65	0.147
	2	52, 262(3)	0.21(3)	0.11(2)	175.224	51,872–52,555	60	
	3	52, 979(3)	0.29(2)	0.17(1)	117.119	52,555–53,273	49	
	4	54, 433(20)	0.61(5)	0.29(3)	134.758	54,058–54,782	28	
	5	55,105(23)	0.64(1)	–0.010(8)	42.826	54,782–55,461	18	
	6	55,487(13)	0.64(2)	0.06(1)	97.024	55,105–55,859	27	
J1847–0402	1	52, 028(3)	0.09(2)	–0.06(1)	62.157	51,550–52,300	24	0.183
J1853+0545	1	54, 199(4)	0.109(5)	0.70(3)	78.022	53,500–55,110	53	3.27
J1909+1102	1	54,659(1)	0.12(2)	1.23(2)	68.666	54,400–54,958	21	1.70
J1957+2831	1	56,268(12)	0.37(9)	0.06(4)	789.092	54,800–56,718	54	1.57
J2219+4754	1	52,454(9)	0.18(1)	0.4(1)	64.625	52,102–52,874	37	3.09
	2	55,012(3)	0.068(3)	–0.08(3)	38.938	54,004–55,496	44	
J2225+6535	1	54, 668(3)	0.30(1)	1.57(7)	63.626	54,300–55,028	22	1.12
	2	56142(1)	1.65(2)	1.54(7)	54.965	55,761–56,487	13	

Figure 1(a) shows the spin-down rate ($|\dot{\nu}|$) of post-glitch is larger than the pre-glitch.

3.2. PSR J1705–3423 (B1705–3423)

PSR B1705–3423 was first found in the Parkes Southern Pulsar Survey (Manchester et al. 1996). It possessed a period of 255 ms and the periodic first derivative of 1.076×10^{-15} , which implies a characteristic age of 3.76 Myr. Two small glitches had been detected by Espinoza et al. (2011) and Yuan et al. (2010) at MJD $\sim 51,956$ and MJD $\sim 54,408$, respectively. Another new small glitch was discovered at MJD $\sim 55,490$ with a magnitude of $\Delta\nu \sim 1.1 \times 10^{-9}$ Hz. Noted that it is the smallest glitch among the three addressed for the pulsar. Figure 1(b) presents the continuous variations of $\Delta\nu$ and $\dot{\nu}$ of PSR B1705–3423 for 6.2 yr. There is a possible exponential recovery with a timescale of approximately 400 days. There is some sign that the fluctuation of $\dot{\nu}$ after the glitch is greater than that before.

3.3. PSR J1833–0827 (B1830–08)

This pulsar was discovered in a high-radio-frequency survey for distant pulsars carried out at Jodrell Bank (Clifton & Lyne 1986). PSR J1833–0827 owns a period of 85 ms and a period derivative of 9.18×10^{-15} giving it a young characteristic age of 147 kyr. This pulsar suffered a giant glitch of fractional size $\Delta\nu/\nu = 1.9 \times 10^{-6}$ and $\Delta\dot{\nu}/\dot{\nu} = 1.7 \times 10^{-3}$ in June 1990 (Shemar & Lyne 1996). Espinoza et al. (2011) reported another one with an amplitude of $\Delta\nu/\nu = 0.9 \times 10^{-9}$ at MJD $\sim 47,541$. Six new small glitches have been detected in this pulsar after MJD $\sim 48,051$, which makes it another frequent glitching pulsar. The relative changes of the rotational frequency $\Delta\nu/\nu$ shown in Figures 1(c)–(h) ranges from 0.21×10^{-9} to

0.64×10^{-9} . Figures 1(c) and 1(d) show the spin-down rate $|\dot{\nu}|$ of post-glitches are larger than the pre-glitches. There is likely a linear decay of pulse frequency ν relative to the pre-glitch and over-recoveries in Figures 1(e) and (f), while $\Delta\nu$ is almost unchanged in Figures 1(g) and (h) after glitches. A gap lasting for ~ 100 days exists in glitches shown in Figures 1(f) and 1(g). Besides, both Figures 1(e) and (f) show the $\dot{\nu}$ fluctuations of post-glitches are greater than pre-glitches.

3.4. PSR J1847–0402 (B1844–04)

PSR J1847–0402 was discovered in a systematic search at low galactic latitudes near the center frequency of 408 MHz using the Mark I radio telescope at Jodrell Bank (Davies et al. 1970). The pulsar owns a period of 598 ms and a modest period derivative ($\dot{P} \sim 5.17 \times 10^{14}$), implying a relatively young pulsar with a characteristic age of about 183 kyr. Two small glitches were detected for PSR B1844–04 around MJD $\sim 55,502$ and $58,244$ with $\Delta\nu/\nu \sim 10^{-10}$ (Lower et al. 2021; Basu et al. 2022). Figure 1(i) shows another new small glitch at MJD $\sim 52,028$. It is seemingly that there exists a recovery of similar exponential function of a small part of the variation in rotation frequency ν with a timescale of approximately 60 days.

3.5. PSR J1853+0545 (B1853+0545)

PSR J1853+0545 was found in the Parkes Multi-beam Pulsar Survey-III (Kramer et al. 2003). It possesses a period of 126 ms and a small period derivative ($\dot{P} \sim 6.12 \times 10^{-16}$), indicating a relatively larger characteristic age τ_c of 3.27 Myr. Yuan et al. (2010) detected the first glitch with a small size of $\Delta\nu/\nu = 1.46 \times 10^{-9}$, following an exponential recovery with fractional decay $Q = 0.22$. Figure 1(j) presents another new small glitch measured at MJD $\sim 54,199$. Similar to PSR J0528

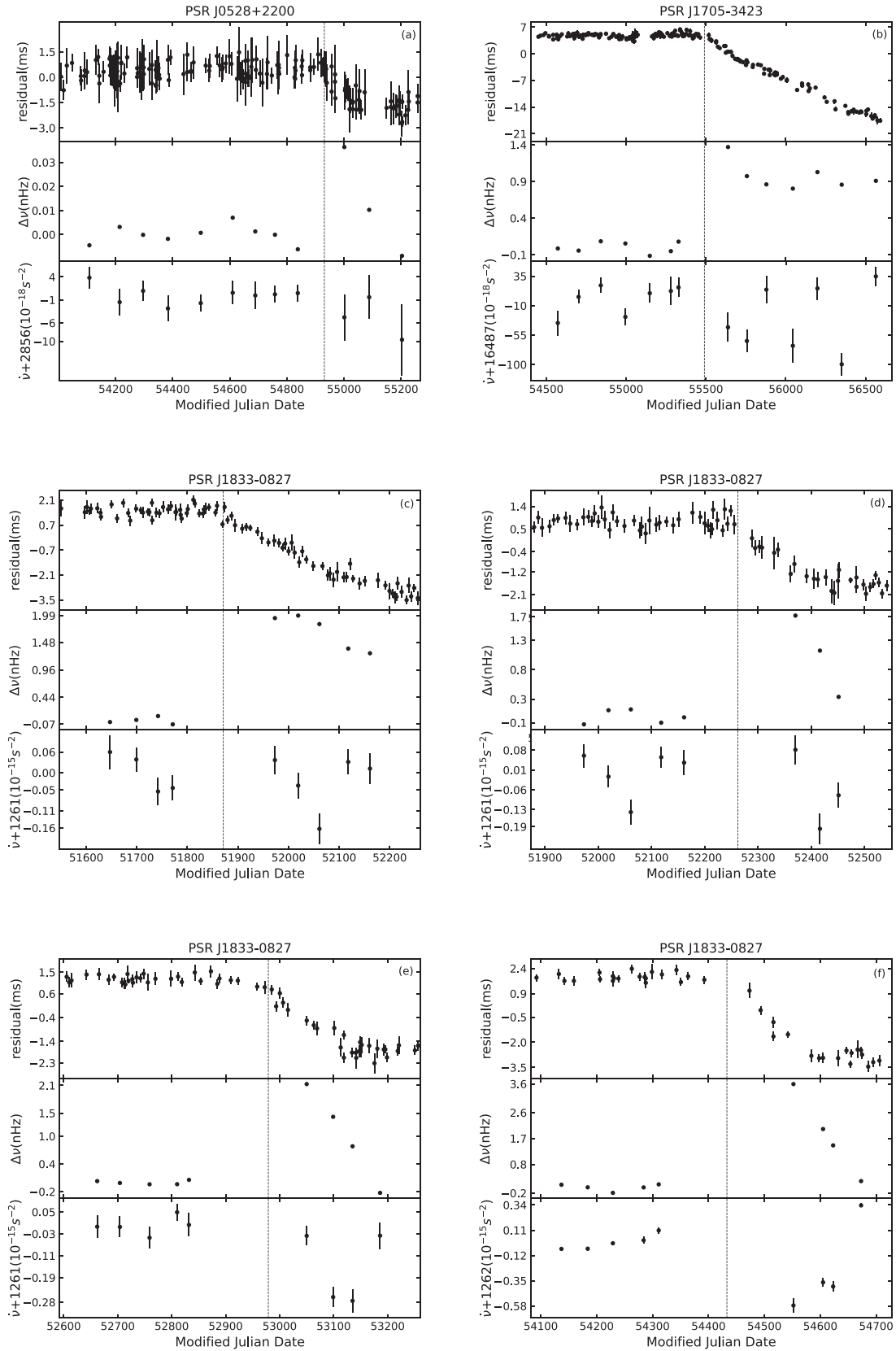


Figure 1. Sixteen glitches in nine pulsars. The top panel of each subplot shows timing residuals relative to the pre-glitch model. The center panel is the variations of rotational frequency $\Delta\nu$ relative to the pre-glitch solutions. The bottom panel shows the variations of the first derivative of frequency $\dot{\nu}$. The vertical dashed lines denote the glitch epochs within our data span.

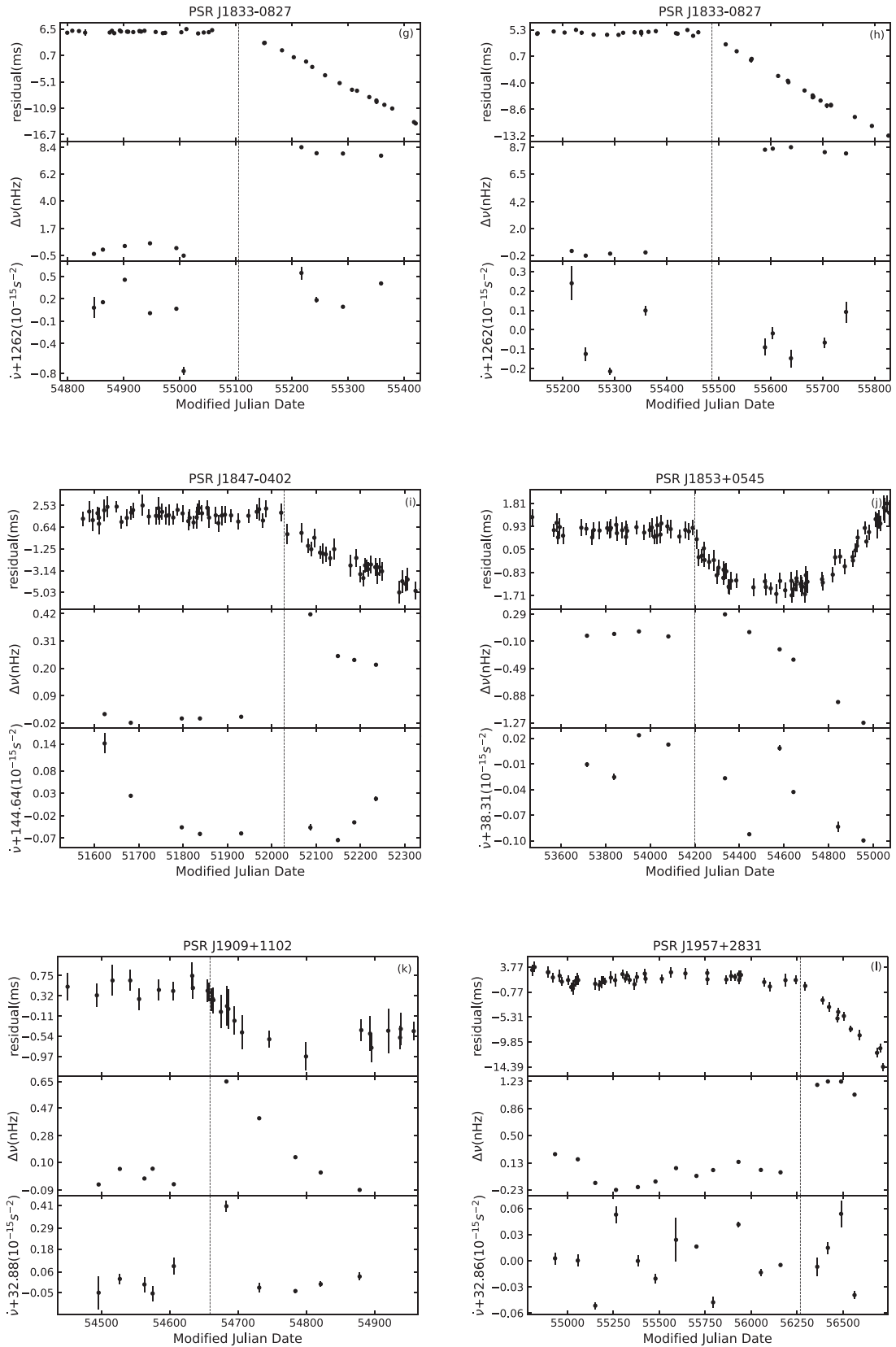


Figure 1. (Continued.)

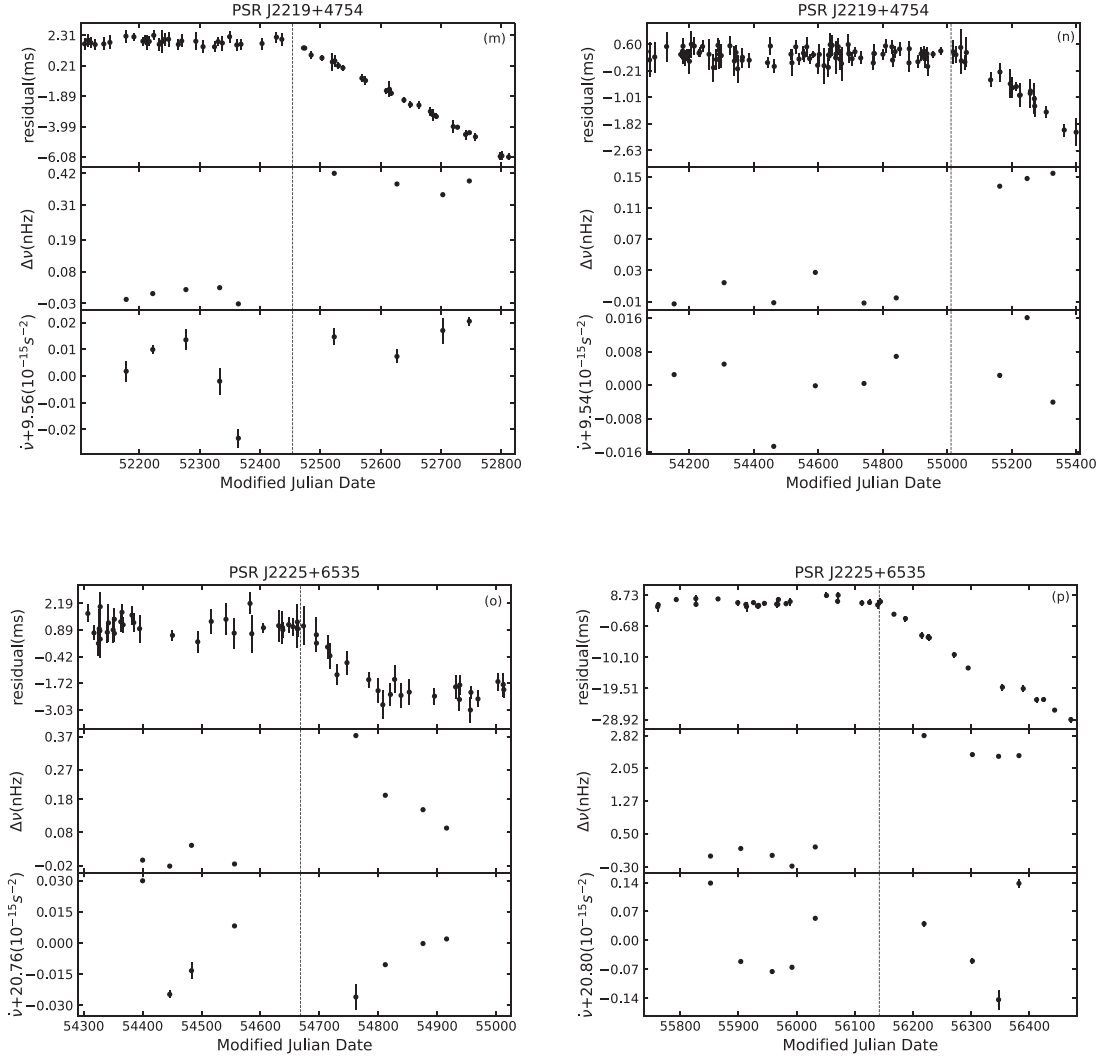


Figure 1. (Continued.)

+2200, there is possibly an over-recovery and a linear decay of ν relative to the pre-glitch solutions which lasts more than 600 days. A second time, this is similar to the Crab pulsar post glitch behavior (Lyne et al. 1993). The bottom panel of Figure 1(j) shows a noticeable fluctuation in $\dot{\nu}$ after the glitch.

3.6. PSR J1909+1102 (B1907+10)

PSR J1847–0402 was discovered in a systematic search at low galactic latitudes, using the Mark I radio telescope and a radio frequency of 408 MHz (Davies et al. 1972, 1973). This pulsar possesses a period of 0.284 s and is relatively old. Yuan et al. (2010) found a minor glitch at MJD 52,700 with $\Delta\nu/\nu \sim 2.7 \times 10^{-10}$. Afterwards, there exists another glitch detected by us at MJD $\sim 54,659$, with the magnitude of 0.12×10^{-9} . The post-glitch behaviors of $\dot{\nu}$ and $\Delta\nu$ are shown in

Figure 1(k) and are similar to that of the glitch in Figure 1(j). The spin-down rate $|\dot{\nu}|$ has a larger size after the glitch than that before. The fluctuation of $\dot{\nu}$ before the glitch is smaller than that after.

3.7. PSR J1957+2831

PSR J1957+2831 was found during the search of the supernova remnants G65.1+0.6 with the 76 m Lovell radio telescope at Jodrell Bank (Lorimer et al. 1998). It possesses a period of 308 ms and $\tau_c \sim 1.57$ Myr. A new minor glitch with $\Delta\nu/\nu \sim 0.37 \times 10^{-9}$ was detected at MJD $\sim 56,278$. This glitch is the fourth jump event in frequency for PSR J1957+2831 after three glitches were reported by Espinoza et al. (2011). Figure 1(l) shows that no remarkable variations in spin-down rate ($\dot{\nu}$) can be related to this glitch. This event leads to a

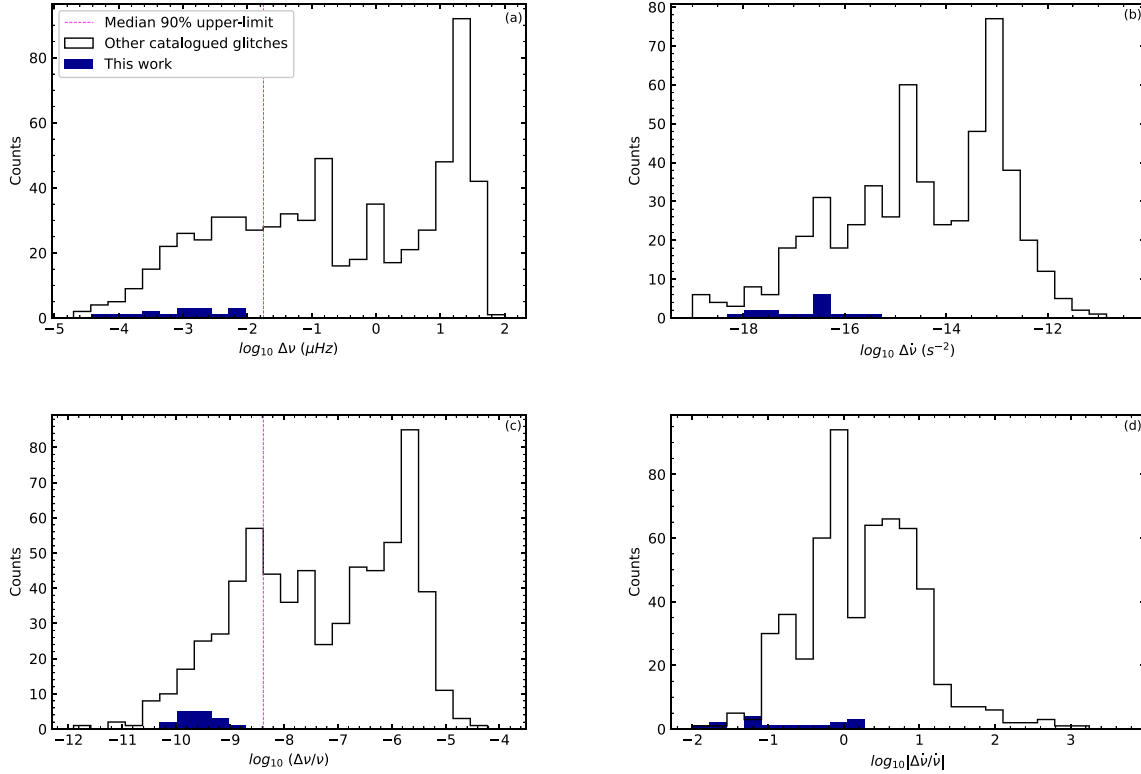


Figure 2. Histograms of $\Delta\nu$, $\Delta\dot{\nu}$, $\Delta\nu/\nu$, and $\Delta\dot{\nu}/\dot{\nu}$ for the 16 glitches in our sample (navy) and the JBO glitch catalog after removing those listed in Table 1 (black). The dashed fuchsia lines in panels (a) and (c) show the median upper limit on the glitch size after averaging across our sample.

raise in frequency ν with $\Delta\nu \sim 1.5$ nHz. The fluctuation of $\dot{\nu}$ is similar before and after the glitch.

3.8. PSR J2219+4754 (B2217+47)

This pulsar was discovered during a search for pulsar survey carried out with the 300-foot transit telescope at the US National Radio Astronomy Observatory in October and November 1968 (Taylor & Huguenin 1969). It is a slow pulsar with a P of 538 ms, and Michilli et al. (2018) had presented a comprehensive study of profile variations in PSR B2217+47. PSR J2219+4754 is relatively old ($\tau_c \sim 3.09$ Myr). Basu et al. (2022) observed a glitch at MJD $\sim 55,857$ with a magnitude $\Delta\nu/\nu \sim 1.16 \times 10^{-9}$. We measured two new glitches in this work. Figure 1(m) shows the same trend between frequency increment and spin-down rate of post-glitch. There is probably a continued increment in the frequency ν relative to the extrapolated pre-glitch that lasts more than 300 days, as shown in Figure 1(n). This is unusual for post-glitch behavior. Such behavior has also been seen for PSR J0147+5922 at MJD $\sim 53,682$ (Yuan et al. 2010).

3.9. PSR J2225+6535 (B2224+65)

PSR J2225+6535 was found in a low latitude pulsar survey using the Mark 1A radio telescope at Jodrell Bank observed in

1972 (Davies et al. 1973). The pulsar is a slow-spin ($P \sim 683$ ms) NS (Cordes et al. 1993), traveling at $\sim 800\text{--}1600$ K ms^{-1} in Guitar Nebula (Chatterjee & Cordes 2004). It seems to be a young pulsar with a characteristic age of about 1.1 Myr. We measured two small glitches after five glitches addressed by Backus et al. (1982); Janssen & Stappers (2006) and Yuan et al. (2010), respectively. Among the five previous glitches, only the first one is a large glitch with $\Delta\nu/\nu \sim 1.7 \times 10^{-6}$ at MJD $\sim 43,072$ (Backus et al. 1982). As seen in Figure 1(o), there is the possibility of a short timescale (~ 50 days) exponential recovery in $\dot{\nu}$. Although the data span of post-glitch in Figure 1(p) is short, it is likely that there exists a partial exponential recovery change in frequency after the jump, but it cannot recover to the trend before the glitch. This behavior is very homologous with which detected in the Vela pulsar (Lyne et al. 1996). Compared to the pre-glitch, no or little change in post-glitch $\dot{\nu}$ was observed.

4. Discussion

4.1. Glitch Size

These nine pulsars are all isolated stars with characteristic ages ranging from 0.147 to 3.76 Myr. Large glitches are mainly limited to pulsars with characteristic ages τ_c less than 10^5 yr. Therefore, it is not surprising that all 16 glitches show a small fractional size. Such glitches are difficult to detect for Parkes

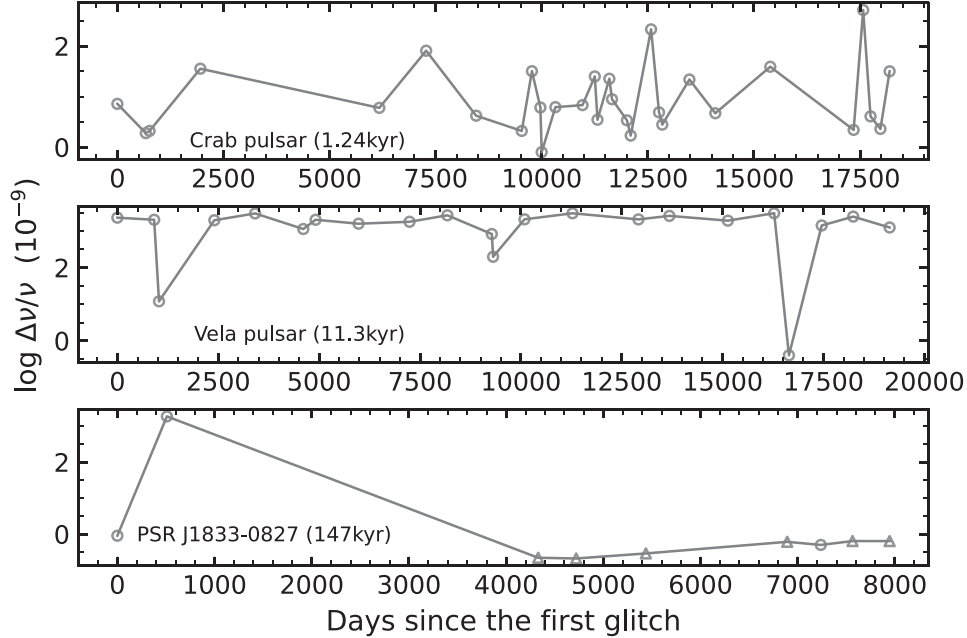


Figure 3. The time series of glitches for PSR J1833–0827, Vela and Crab pulsars. The characteristic age of each pulsar is shown in parentheses. Data from the glitch table of the JBO pulsar catalog (<https://www.jb.man.ac.uk/pulsar/glitches/gTable.html>) are shown by circles, as those in our sample are denoted by triangles.

and Jodrell Bank Observatory and have been missed before (Yu et al. 2013). This could possibly attribute to the high cadence of our observations. The bimodal distribution of the detected fractional glitch sizes was previously studied and reported by several astronomers (Espinoza et al. 2011). As displayed in Figure 2(c), the first peak of the distribution was around 2×10^{-9} and the second peak lies around 10^{-6} . As mentioned by Espinoza et al. (2011), the left edge of the bimodal distribution is significantly limited by observational selection. The realistic number of small glitches could be large in the intrinsic distribution. Our observations entirely contribute to the left part of the first peak. The dip at $\Delta\nu/\nu \sim 10^{-7}$ indicates that there might be two mechanisms which could generate a glitch event. It has been proposed that large glitches may be caused by the abrupt move of angular momentum from a crustal superfluid to the rest of the star, whereas starquakes given rise by the cracking of stellar crust may induce minor glitches. The fractional size of glitch depends on both the glitch size and the spin frequency ν of the pulsar. As shown in Figure 2(a), $\Delta\nu$ also has a bimodal distribution. However, the peak for large glitches is narrower in $\Delta\nu$ than $\Delta\nu/\nu$.

Figure 3 shows the time sequence of fractional glitch sizes for PSR J1833–0827, a new frequent glitch pulsar, Crab pulsar, and Vela pulsar. Most glitches in the PSR B0833–45 (Vela) are large with similar amplitude, but lots of smaller glitches were seen accidentally. There are plenty of small glitches and only one large for PSR J1833–0827; similar behaviors are also seen in J1740–3015, PSRs J1341–6220,

J0631+1036, and J1801–2304. Figure 4 shows the connection between the median $\Delta\nu$ ($\Delta\nu_m$) and average $\Delta\nu$ ($\langle \Delta\nu \rangle$) which indicates the skewness of glitch size for a certain pulsar. Pulsars with symmetrical glitch size distributions will fall on the diagonal line, corresponding to outliers and considered to be those that lie more than one standard deviation (SD) from the straight line and are labeled as a star. Outliers shown in Figure 4 are pulsars that suffer small size glitches but also occasional large glitches. This is consistent with the results from Basu et al. (2022).

4.2. Spin-down Rate Change

The change in the rotation frequency during a glitch is usually accompanied by a variation in the spin-down rate. Negative values of $\Delta\dot{\nu}$ are seen in the majority of glitches, although the inferred change in the spin-down rate can be either positive or negative. The distribution of $\Delta\dot{\nu}$ is shown in Figure 2(b). The distribution is also bimodal, and our results entirely contribute to the left peak, as was the situation for the distribution of glitch size. The spin-down rate change in $\Delta\dot{\nu}$ significantly correlates with glitch size (Basu et al. 2022). Therefore, the spin-down rate changes shown in Figure 2(b) are also very small.

4.3. Glitch Rate

The glitch rate (R_g) is a useful parameter to estimate how dynamic a pulsar was in terms of glitches. This rate might

Table 2
Observation Times Span and Glitch Rate of Nine Pulsars Observed at Jodrell Bank Observatory (JBO) or Nanshan Having Glitched

PSR J	Range (MJD)		No. of Glitches		Glitch Rate (R_g , yr $^{-1}$)	
	JBO	Nanshan	JBO	Nanshan	JBO	Nanshan
J0528+2200	45010–58482	51547–56719	4	4	0.11(5)	0.28(14)
J1705+3423	49086–58482	52485–56719	3	2	0.12(7)	0.17(12)
J1833–8273	46449–58482	51549–56719	3	7	0.09(5)	0.49(19)
J1847–0402	44816–58482	51550–56719	3	3	0.08(5)	0.21(12)
J1853+0545	51634–58482	52497–56719	1	2	0.05(5)	0.17(12)
J1909+1102	44816–58482	52470–56719	1	2	0.03(3)	0.17(12)
J1957+3831	50239–58482	52503–56719	3	3	0.13(8)	0.26(15)
J2219+4754	45953–58482	51549–56719	1	3	0.03(3)	0.21(12)
J2225+6535	44817–58482	52470–56719	4	5	0.11(5)	0.43(19)

Note. The beginning and end data of JBO refer to Espinoza et al. (2011) and Basu et al. (2022), respectively.

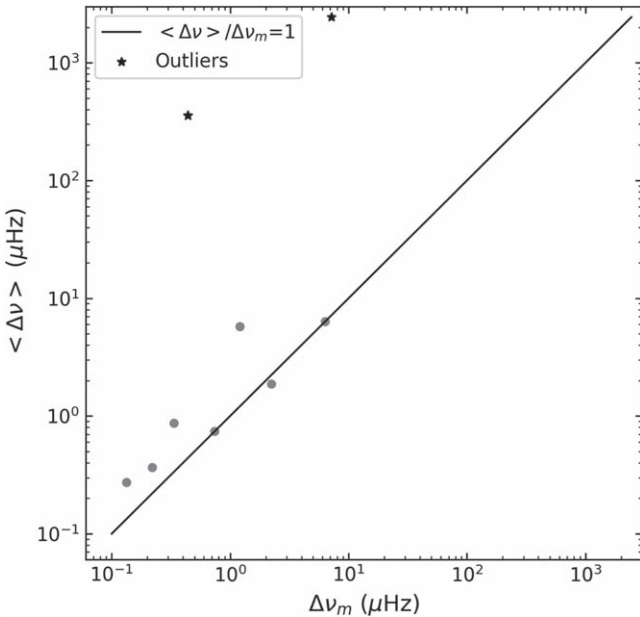


Figure 4. The average glitch size $\langle \Delta\nu \rangle$ vs. the median glitch size $\Delta\nu_m$ of nine pulsars are shown as gray points. The marked star points indicate the nine pulsars with a skewed $\Delta\nu$ distribution, and the diagonal line (black) follows the relation $\langle \Delta\nu \rangle = \Delta\nu_m$.

change over the years of observations. The glitch rates are calculated assuming that they are constant in time and should be treated as approximate values. The glitch rate ($R_g = N/T$) can be defined as where N is the total number of observed glitches, and T is the time interval of observations at the Nanshan and Jodrell Bank Observatory (JBO). The uncertainty on the glitch rates was computed as the square root of total number N divided by the data span. The glitch rate of the nine pulsars derived from the JBO and Nanshan is listed in Table 2. Our data spans are shorter than that of JBO. But the number of glitches we detected is larger than JBO for five pulsars. All the

glitch rates obtained from Nanshan are higher than that of JBO. This could possibly be attributed to the high cadence of our observations.

5. Conclusion

In this paper, we reported glitches in the timing residuals of nine pulsars. Sixteen new glitches have been identified in these nine pulsars. Glitches have been reported for all nine pulsars before. All 16 glitches show a small fractional size. Some of the 16 glitches may have exponential or linear recovery, but it is challenging for us to make further analyses under the large gap in the data set. The timing accuracy, intrinsic timing noise, and observational sampling noise may also hinder the detection of post-glitch recoveries in very short terms. All the glitch rates obtained from Nanshan are higher than that from the Jodrell Bank Observatory. Most known glitches are published by JBO and Parkes. However, such glitches are difficult to detect for Parkes and JBO, and the absolute number of small glitches can be large. We also found that PSR J1833–0827 is a frequently glitching pulsar with many minor glitches. All the glitch rates obtained from Nanshan are higher than that of JBO. The high glitch rate and small glitch size could possibly result from the high observation cadence. About 300 pulsars have been observed with the Nanshan 26 m telescope for more than ten years. We have processed nearly 60 pulsars, and about a quarter of them have been shown to glitch. The timing results of the other pulsars will be presented in the future.

Acknowledgments

The authors wish to thank Dr. Richard N. Manchester and Dr. G. Hobbs for their valuable suggestions and comments. This work is supported by the National SKA Program of China (No. 2020SKA0120100), the National Natural Science Foundation of China (NSFC, No. 12041304), Youth Innovation Promotion Association of the Chinese Academy of Sciences, the CAS Jianzhijia project, Guizhou Provincial Science and

Technology Foundation (No. ZK[2022]304), and Heaven Lake Hundred-Talent Program of Xinjiang Uygur Autonomous Region of China.

References

- Backus, P. R., Taylor, J. H., & Damashek, M. 1982, *ApJL*, **255**, L63
- Basu, A., Shaw, B., Antonopoulou, D., et al. 2022, *MNRAS*, **510**, 4049
- Baym, G., & Pethick, C. J. 1996, *PhRvL*, **76**, 6
- Bransgrove, A., Beloborodov, A. M., & Levin, Y. 2020, *ApJ*, **897**, 173
- Chamel, N. 2013, *PhRvL*, **110**, 011101
- Chatterjee, S., & Cordes, J. M. 2004, *ApJL*, **600**, L51
- Clifton, T. R., & Lyne, A. G. 1986, *Natur*, **320**, 43
- Cordes, J. M., Romani, R. W., & Lundgren, S. C. 1993, *Natur*, **362**, 133
- Cordes, J. M., & Shannon, R. M. 2010, arXiv:1010.3785
- Davies, J. G., Large, M. I., & Pickwick, A. C. 1970, *Natur*, **227**, 1123
- Davies, J. G., Lyne, A. G., & Seiradakis, J. H. 1972, *Natur*, **240**, 229
- Davies, J. G., Lyne, A. G., & Seiradakis, J. H. 1973, *NPhS*, **244**, 84
- Downs, G. S. 1982, *ApJL*, **257**, L67
- Espinoza, C. M., Lyne, A. G., Stappers, B. W., & Kramer, M. 2011, *MNRAS*, **414**, 1679
- Folkner, W. M., Williams, J. G., & Boggs, D. H. 2009, Interplanetary Network Progress Report, 42
- Groth, E. J. 1975, *ApJS*, **29**, 443
- Gügercinoğlu, E., & Alpar, M. A. 2014, *ApJL*, **788**, L11
- Haskell, B., & Melatos, A. 2015, *IJMPD*, **24**, 1530008
- Hobbs, G., Dai, S., Manchester, R. N., et al. 2019, *RAA*, **19**, 020
- Hobbs, G., Edwards, R., & Manchester, R. 2006, *ChJAS*, **6**, 189
- Hobbs, G., Jenet, F., Lee, K. J., et al. 2009, *MNRAS*, **394**, 1945
- Hobbs, G., Lyne, A. G., & Kramer, M. 2010, *MNRAS*, **402**, 1027
- Hotan, A. W., Bailes, M., & Ord, S. M. 2004, *MNRAS*, **355**, 941
- Janssen, G. H., & Stappers, B. W. 2006, *A&A*, **457**, 611
- Kaspi, V. M., & Beloborodov, A. M. 2017, *ARA&A*, **55**, 261
- Kerr, M., Reardon, D. J., Hobbs, G., et al. 2020, *PASA*, **37**, e020
- Kramer, M., Bell, J. F., Manchester, R. N., et al. 2003, *MNRAS*, **342**, 1299
- Kramer, M., Stairs, I. H., Manchester, R. N., et al. 2006, *Sci*, **314**, 97
- Kramer, M., Stairs, I. H., Manchester, R. N., et al. 2021, *PhRvX*, **11**, 041050
- Lorimer, D. R., Lyne, A. G., & Camilo, F. 1998, *A&A*, **331**, 1002
- Lower, M. E., Johnston, S., Dunn, L., et al. 2021, *MNRAS*, **508**, 3251
- Lyne, A., Hobbs, G., Kramer, M., Stairs, I., & Stappers, B. 2010, *Sci*, **329**, 408
- Lyne, A. G., Pritchard, R. S., & Graham Smith, F. 1993, *MNRAS*, **265**, 1003
- Lyne, A. G., Pritchard, R. S., Graham-Smith, F., & Camilo, F. 1996, *Natur*, **381**, 497
- Manchester, R. N., Hobbs, G. B., Hobbs, M., & Teoh, A. 2005, *AJ*, **129**, 1993
- Manchester, R. N., Lyne, A. G., D'Amico, N., et al. 1996, *MNRAS*, **279**, 1235
- Michilli, D., Hessels, J. W. T., Donner, J. Y., et al. 2018, *MNRAS*, **476**, 2704
- Parthasarathy, A., Shannon, R. M., Johnston, S., et al. 2019, *MNRAS*, **489**, 3810
- Shannon, R. M., & Cordes, J. M. 2017, *MNRAS*, **464**, 2075
- Shaw, B., Stappers, B. W., & Weltevrede, P. 2018, *MNRAS*, **475**, 5443
- Shemar, S. L., & Lyne, A. G. 1996, *MNRAS*, **282**, 677
- Staelin, D. H., & Reifenstein, E. C. I 1968, *Sci*, **162**, 1481
- Taylor, J. H., & Huguenin, G. R. 1969, *Natur*, **221**, 816
- Wang, N., Wu, X.-J., Manchester, R. N., et al. 2001, *ChJAA*, **1**, 195
- Yu, M., Manchester, R. N., Hobbs, G., et al. 2013, *MNRAS*, **429**, 688
- Yuan, J. P., Wang, N., Manchester, R. N., & Liu, Z. Y. 2010, *MNRAS*, **404**, 289